微生物学通报
Microbiology China
tongbao@im.ac.cn
http://journals.im.ac.cn/wswxtbcn

Dec. 20, 2021, 48(12): 4564−4580
DOI: 10.13344/j.microbiol.china.210306

研究报告

Proteome analysis and heterologous cargo delivery of *Vibrio natriegens* outer membrane vesicles

CUI Yang DONG Tao*

School of Life Sciences and Biotechnology, Shanghai Jiao Tong University, Shanghai 200240, China

Abstract: [Background] The fast-growing Gram-negative bacterium *Vibrio natriegens* is a burgeoning tool in biotechnology. Previous research has mainly focused on developing tools for *in vitro* and *in vivo* recombinant protein production using *V. natriegens*. However, many physiological activities that support fast growth and protein production remain largely uncharacterized. Ubiquitously produced by bacteria, outer membrane vesicles (OMVs) not only carry out important functions but also can serve as a useful delivery tool for vaccine and therapeutics development. **[Objective]** Characterize the proteomes of OMVs during exponential phase growth and to employ OMVs for heterologous protein delivery. **[Methods]** Using transmission electron microscopy, dynamic light scattering, and mass spectrometry, we characterized the morphology and size distribution of extracted OMVs and their protein composition. We used the superfolded green fluorescent protein (sfGFP) as cargo to determine OMVs protein carriers. **[Results]** OMVs of mid- and late-exponential phases cultures contain 288 and 317 proteins, respectively. These proteins belong to multiple functional groups including ABC transporters, flagella and two-component systems. By contrast, we identified 1 480 and 1 565 proteins in whole cell samples under these two conditions, respectively. We screened OMV proteins for candidate carriers and found an OmpA-family protein that we name OmpA24 could enrich the sfGFP as a protein-fusion cargo in OMVs. **[Conclusion]** We demonstrate for the first time that *V. natriegens* can produce OMVs throughout exponential growth and present the first proteomic snapshot of OMVs and related whole cell samples under different growth phases. OmpA24 protein is a promising carrier for delivery of heterologous protein-fusion cargo into OMVs. This study will facilitate the application of *V. natriegens* in protein expression and OMV-mediated secretion.

Keywords: *Vibrio natriegens*, outer membrane vesicles, biotechnology

Foundation items: National Key Research and Development Program of China (2020YFA0907202); National Natural Science Foundation of China (31770082, 32030001)
***Corresponding author:** Tel: 86-21-34205709; E-mail: tdong@sjtu.edu.cn
Received: 26-03-2021; **Accepted:** 07-05-2021; **Published online:** 10-05-2021
基金项目：国家重点研发计划(2020YFA0907202)；国家自然科学基金(31770082，32030001)
*通信作者：Tel：021-34205709；E-mail：tdong@sjtu.edu.cn
收稿日期：2021-03-26；接受日期：2021-05-07；网络首发日期：2021-05-10

需钠弧菌外膜囊泡的蛋白质组分析与异源蛋白的递送

崔阳 董涛*

上海交通大学生命科学技术学院 上海 200240

摘 要:【背景】需钠弧菌(*Vibrio natriegens*)是一种快速生长的革兰氏阴性菌，作为一种新兴工具在生物技术领域有重要的应用潜力。此前的研究主要集中在开发利用 *V. natriegens* 成为体内外重组蛋白生产的工具。然而，许多支持细菌进行快速生长和蛋白质生产的生理活动大部分仍未确定。外膜囊泡(Outer Membrane Vesicle，OMV)是由革兰氏阴性细菌普遍产生的一种球形小泡，其不仅具有重要的功能，而且还可以作为一种应用于疫苗治疗的高效运载工具。【目的】表征指数生长期 OMV 的蛋白质组并利用 OMV 进行异源蛋白的递送。【方法】使用透射电镜、动态光散射和质谱学的方法，观察 OMV 的形态及粒径分布并鉴定蛋白组成。以超折叠绿色荧光蛋白(Superfolded Green Fluorescent Protein，sfGFP)作为货物蛋白来确定 OMV 蛋白载体。【结果】从细菌培养的指数期中期和末期分别提取的 OMV 中鉴定到了 288 个和 317 个蛋白。这些蛋白分属不同的功能组，包括 ABC 转运蛋白、鞭毛、双组分系统。相比之下，同时鉴定了全细胞样品，其在指数期中期和末期分别含有 1 480 个和 1 565 个蛋白。我们筛选 OMV 的蛋白作为候选载体发现了一种属于 OmpA 家族的蛋白(命名为 OmpA24)，其能够将 sfGFP 以融合货物蛋白的形式运载到 OMV 中。【结论】首次证实 *V. natriegens* 能够在指数生长期产生 OMV，并展示了第一个不同生长时期 OMV 和全细胞的蛋白质组鉴定结果。OmpA24 是将外源融合货物蛋白呈递到 OMV 中的有前景的载体。本研究有助于促进 *V. natriegens* 在蛋白表达和 OMV 介导的分泌中的应用。

关键词: 需钠弧菌，外膜囊泡，生物技术

Protein expression using the common lab strains of *Escherichia coli* and *Pichia pastoris* is a key pillar of biotechnology, supporting not only basic research but also pharmaceutical development and biomaterial manufacturing[1-2]. Recently, a fast-growing *Vibrio natriegens* strain Vmax has been engineered as an additional tool with great potential for producing heterologous proteins[3]. Due to its fastest growth rate and compatibility with existing expression tools, *V. natriegens* Vmax has attracted increasing attention focused on genetic engineering and optimizing cytoplasmic expression conditions. These studies include genome engineering[4], CRISPR-Cas9 editing[5], expression of natural products and multisubunit membrane proteins[6-7], as well as the development of a cell-free protein synthesis system[8]. However, many physiological aspects of *V. natriegens* are still not fully understood, hindering its application[9].

Bacterial growth in batch culture exhibits distinct growth phases including lag, exponential, stationary, and long-term stationary phases[10-13]. Heterologous protein expression is often induced during the exponential phase in which protein expression machinery is expected to function at the highest levels. Although the growth rate of cells remains nearly constant in exponential phase, studies in *E. coli* have demonstrated that cellular physiological states are not constant but actively changing in response to nutrient depletion and metal availability during growth[14]. What is the protein expression profiles during the rapid growth of *V. natriegens* still unknown due to the unexamined proteome.

Outer membrane vesicles (OMVs) are spherical vesicles with a diameter of about 20−250 nm that are ubiquitously secreted by Gram-negative bacteria and enclose outer membrane proteins, periplasmic proteins, lipopolysaccharide, cytoplasmic proteins, outer membrane lipids, DNA, RNA and some virulence factors[15-20]. OMVs play important roles in many biological processes, including nutrient and iron acquisition, stress response, interbacterial communication, and pathogenesis[21-25]. In addition, OMVs have been used as vaccine candidates and for

therapeutic delivery due to their safety and similar immunogenic properties to whole cells[26-27]. Heterologous expression of antigens in OMVs is a common strategy for producing engineered OMV vaccines, and target proteins are often fused with vesicle-associated proteins, including ClyA, AIDA and Hbp, for packaging into the OMVs[28-30]. Proteomic analyses have been used to determine the composition of OMVs in many bacteria, including *Fusobacterium nucleatum*[31], *Pseudomonas syringae*[32], *Helicobacter pylori*[33], *Campylobacter jejuni*[34], *Xanthomonas campestris* pv. campestris[35], *Acinetobacter baumannii*[36], and *E. coli*[37]. However, the OMVs in *V. natriegens* have not been characterized.

In this study, we report the proteomic characterization of whole cell and OMVs at mid-log (OD_{600}=0.5) and late-log (OD_{600}=1.5) growth phases of *V. natriegens* strain Vmax. By LC-MS/MS analysis, we identified hundreds of proteins in various physiological pathways in both the whole cell and OMV samples. We also screened some OMV proteins that were present in both mid- and late-log growth phases and demonstrate that an OmpA-domain protein carrier, OmpA24, can deliver a heterologous protein sfGFP (superfolded green fluorescent protein) as a protein-fusion cargo to the OMVs. Collectively, our results provide the first snapshot of protein expression in the whole cell and OMVs during fast growth of *V. natriegens* and found an efficient protein carrier. The results will facilitate further studies of *V. natriegens* and its OMVs for both understanding physiological functions and for biotechnological applications.

1 Materials and Methods

1.1 Main reagents and equipment

Mouse monoclonal anti-GFP antibody, Abcam; ECL solution, Bio-Rad; goat anti-mouse IgG HRP, Golden Bridge Biotechnology limited company; RpoB antibody, Biolegend. Filter, Jet Bio-Filtration limited company; Amicon Ultra-4 centrifugal filter, Millipore; ultracentrifuge, Beckman Instruments; transmission electron microscope, FEI company; Zetasizer Nano S, Malvern instruments limited company; Q-Exactive mass spectrometer and Easy nLC HPLC system, Thermo Scientific; inverted microscope, Nikon corporation instruments company.

1.2 Bacterial strains and growth conditions

All the strains and plasmids used in this study are listed in Table 1. The *V. natriegens* strain Vmax contains a T7 RNA polymerase-mediated expression system[3]. Bacterial cultures were grown in LB3 medium (Lysogeny Broth with 3% (*W/V*) final NaCl) for *V. natriegens* and LB for *E. coli* strains[3]. Ampicillin (100 μg/mL) and IPTG (0.001 mmol/L or

Table 1 Strains and plasmids used in this study
表 1 本文用到的菌株和质粒

Strains or plasmids	Description	References
V. natriegens Vmax express	A T7 expression cassette is integrated in chromosome	[3]
E. coli T-Fast	F–*proA*$^{+}$B^{+}*lacIq* Δ*lacZM15*/*fhuA2* Δ(*lac-proAB*) *glnV galK16 galE15* R(*zgb-210*::*Tn10*)*TetS endA1 thi-1* Δ(*hsdS-mcrB*)*5*	Lab stock
psfGFP	pET-22b vector for expressing sfGFP with a C-terminal 6×His tag, IPTG inducible	Lab stock
pOmpW	pET-22b vector for expressing OmpW-sfGFP fusion with a C-terminal 6×His tag, IPTG inducible	This study
pTolC	pET-22b vector for expressing TolC-sfGFP fusion with a C-terminal 6×His tag, IPTG inducible	This study
pOmpA24	pET-22b vector for expressing OmpA24-sfGFP fusion with a C-terminal 6×His tag, IPTG inducible	This study
pPal	pET-22b vector for expressing Pal-sfGFP fusion with a C-terminal 6×His tag, IPTG inducible	This study
pMalE	pET-22b vector for expressing MalE-sfGFP fusion with a C-terminal 6×His tag, IPTG inducible	This study
pTolB	pET-22b vector for expressing TolB-sfGFP fusion with a C-terminal 6×His tag, IPTG inducible	This study
pSkp	pET-22b vector for expressing Skp-sfGFP fusion with a C-terminal 6×His tag, IPTG inducible	This study
pPotD	pET-22b vector for expressing PotD-sfGFP fusion with a C-terminal 6×His tag, IPTG inducible	This study

0.1 mmol/L) were added when needed. To construct the growth curve, overnight cultures were diluted 1:100 into 50 mL LB3 medium in 250 mL conical flask at 37 °C with agitation at 200 r/min. Growth was monitored by taking OD_{600} readings at specific time points as indicated.

1.3 Construction of *V. natriegens* derivative strains

Plasmids were constructed by PCR amplifying the target genes and then ligating to the pET-22b-sfGFP vector through restriction enzymes *Nde* I and *Kpn* I. The expression plasmid of TolB-sfGFP fusion was constructed by Gibson Assembly. All the constructs were verified by sequencing. Primers are listed in Table 2.

1.4 Preparation of whole cell and OMV samples from *V. natriegens*

We used a previously established protocol for isolation of OMVs[38]. Briefly, for wild type bacteria, 5 mL overnight cultures were transferred to 495 mL LB3 broth and grown at 37 °C with 200 r/min shaking. Cultures were grown to mid- and late-exponential phases (OD_{600}=0.5 and 1.5) and the supernatants were collected by centrifugation at 4 500×*g* for 15 min at 4 °C. To further remove residual cells and debris, the collected supernatants were filtered through 0.22 μm pore size filter. EDTA-free protease inhibitors were added to prevent from protein degradation. Filtrates were concentrated by Amicon Ultra-4 centrifugal filter unit with 10 kD molecular weight cut-off and then ultracentrifuged for 3 h at 200 000×*g*, 4 °C. The OMV pellets were resuspended in PBS buffer and stored at −80 °C. Cultures from mid- and late-exponential phases (OD_{600}=0.5 and 1.5) were concentrated or diluted to OD_{600}=1.0. One mL cultures of OD_{600}=1.0 were collected by centrifugation at 2 500×*g* for 8 min at room temperature. Then the pellets were resuspended in SDS-loading buffer and used as whole cell samples followed by SDS-PAGE analysis. For inducing the bacteria carrying pET-22b plasmids, overnight cultures were diluted 1:100 in fresh LB3 with appropriate antibiotics and grown at 37 °C with 200 r/min shaking. Cultures were induced at OD_{600}=0.5 with 0.1 mmol/L or 0.001 mmol/L IPTG for 2 h or 5 h as indicated prior to OMVs isolation.

Table 2 Primers used in this study
表 2 本文用到的引物

Primers	Description	Sequences (5′→3′)
OmpW-*Nde* I-F	Forward primer to amplify *ompW*	ggaattccatatgaaaaaaacaatctgcagtttggcagtg
OmpW-*Kpn* I-R	Reverse primer to amplify *ompW*	ggggtaccaaacttgtaaccaccgctgatcataaatac
TolC-*Nde* I-F	Forward primer to amplify *tolC*	ggaattccatatgaaaaaattgcttccacttttttatcagtgc
TolC-*Kpn* I-R	Reverse primer to amplify *tolC*	ggggtaccgtttacagctttcagacccgcat
OmpA24-*Nde* I-F	Forward primer to amplify *ompA24*. The *Nde* I site is in front of the original start codon of *ompA24*	ggaattccatatgttgaaaaagctgtctatagcacttgctc
OmpA24-*Kpn* I-R	Reverse primer to amplify *ompA24*	ggggtacccttcagaggcaagatttggatttca
Pal-*Nde* I-F	Forward primer to amplify *pal*	ggaattccatatgcaacttaacaaggttctaaaagggctacttatc
Pal-*Kpn* I-R	Reverse primer to amplify *pal*	ggggtaccgtatactaaaaccgcacgacggtttt
MalE-*Nde* I-F	Forward primer to amplify *malE*	ggaattccatatgaaaaagttaagcgctgtagcactaggtac
MalE-*Kpn* I-R	Reverse primer to amplify *malE*	ggggtacctttagtcatttgtttttctgcatcagc
TolB-hifi-F	Forward primer to amplify *tolB*	aagaaggagatatacatatgtttgtactgctaagcagtatgacgaatg
TolB-hifi-R	Reverse primer to amplify *tolB*	cctcctgcggccgcggtacccaaaaacggtgaccacgcag
Skp-*Nde* I-F	Forward primer to amplify *skp*. The *Nde* I site is in front of the original start codon of *skp*	ggaattccatatgttgaataaaatgatcaaagcggctg
Skp-*Kpn* I-R	Reverse primer to amplify *skp*	ggggtacctttagagctttaattacgtcttcagagatgtt
PotD-*Nde* I-F	Forward primer to amplify *potD*	ggaattccatatgaaaagtaaattctacgcaagcgctctat
PotD-*Kpn* I-R	Reverse primer to amplify *potD*	ggggtaccgttgtttacttttagcttttggaagtactcatc
pET-22b-sfGFP-F	Forward confirmation primer of pET-22b-sfGFP vector	cacgatgcgtccggcgtagagg
pET-22b-sfGFP-R	Reverse confirmation primer of pET-22b-sfGFP vector	tttaccgttggttgcatcaccttca

1.5 Transmission electron microscopy (TEM) and dynamic light scattering (DLS)

OMV samples were diluted ten-fold with PBS buffer, and 5 μL was placed on 400-mesh copper grids. For negative staining, samples were stained with 2% uranyl acetate for 40 s, blotted with filter paper and air dried. TEM pictures were examined in a transmission electron microscope at 120 kV acceleration voltage. DLS was performed to determine the size of OMVs by using a Zetasizer Nano S with He-Ne laser (633 nm) at 25 °C by angle of 173 °.

1.6 SDS-PAGE and in-gel digestion

Proteins of whole cell and OMV samples were analyzed by SDS-PAGE (12% acrylamide gel). The gels were stained with Coomassie Blue R-250 and destained by destaining buffer (25% (*V/V*) alcohol, 10% (*V/V*) acetic acid). Gel slices were treated with 200 μL 30% Acetonitrile (ACN) in 100 mmol/L NH_4HCO_3 and then incubated with 10 mmol/L dithiothreitol at 37 °C for 1.5 h. After treatment with 100% ACN for 5 min, 60 mmol/L iodoacetamide was added for the 30 min light-avoidance reaction. Then the samples were incubated with 100 mmol/L NH_4HCO_3 for 15 min at room temperature and treated with 100% ACN for 5 min again. Digestions were performed at 37 °C with 10 ng/μL trypsin for about 20 h. Desalting of digested peptides was performed on C18 Cartridge.

1.7 Liquid Chromatography-Mass Spectrometry (LC-MS/MS)

Mass Spectrometry analysis was performed on the Q-Exactive mass spectrometer coupled with Easy nLC HPLC system. Tryptic peptides were loaded onto the Thermo scientific EASY column (2 cm×100 μm 5 μm-C18), and separated by Thermo scientific EASY column (75 μm×100 mm 3 μm-C18) at 300 nL/min flow rate. Buffer A consisted of 0.1% formic acid in H_2O, and buffer B consisted of 0.1% formic acid in 84% ACN. Peptides were separated and eluted by using the linear gradients of buffer B for 60 min gradient (0%−35% over 50 min; 35%−100% over 50−55 min; 100% over 55−60 min) and for 90 min gradient (0%−55% over 80 min; 55%−100% over 80−85 min; 100% over 85−90 min). The separated peptides were then subjected to the Q-Exactive mass spectrometer for analysis. The detection mode was positive ion mode and the analysis time were 60 min for OMV samples and 90 min for whole cell samples. The parent ion scanning ranged from 300 to 1 800 *m/z* and the first-order mass spectrometry resolution was 70 000 at *m/z* 200. The automatic gain control (AGC) target was 3e6, and the maximum IT was 50 ms. MS2 spectra of the 20 debris maps were acquired after each full scan. The MS2 activation type was HCD. In secondary mass spectrometry, the resolution was 17 500 at *m/z* 200, maximum IT was 60 ms. The microscan was 1, isolation window was 2 *m/z*, normalized collision energy was 27 eV, dynamic exclusion was 60 s and underfill ratio was 0.1%. Proteome Discoverer 1.4 software was used for data analysis. Proteins that appeared in ≥2 trials among the three independent experiments with ≥ one unique peptide (Σ# unique peptides ≥2) and false discovery rate ≤1% were considered reliable protein identification. LC-MS/MS analysis was performed at Shanghai Applied Protein Technology limited company.

1.8 Bioinformatics analysis

Genome sequences of *V. natriegens* ATCC 14048 were searched from GenBank under accession numbers CP016345 and CP016346. For protein identification, the spectra were searched using the proteome data of *V. natriegens* CCUG 16374 from UniProt (www.pir.uniprot.org) database (UP000092577). Subcellular location was analyzed by PSORTb (www.psort.org/psortb/). The functional annotations of identified proteins were defined by the GO and KEGG database. OmpA24 sequence was analyzed with BLASTp to identify homologs and species distribution. In total 20 homologs were manually selected and analyzed by phylogeny together with OmpA24. The phylogenetic tree was constructed using the Maximum-likelihood method in MEGA X software with bootstrap 1 000 iterations, and protein sequences were aligned by MUSCLE algorithms[39]. Domain analysis was performed using PfamScan tool with default settings (https://www.ebi.ac.uk/Tools/pfa/pfamscan/).

1.9 Fluorescence microscopy

Overnight cultures were diluted 1:100 in fresh LB3 with appropriate antibiotics and grown at 37 °C with 200 r/min shaking. Cells were induced when OD_{600}=0.5 with 0.1 mmol/L or 0.001 mmol/L IPTG for 2 h or 5 h. Cultures were then centrifuged for

8 min at 2 500×*g*, concentrated to OD_{600}=10.0 and resuspended in 1×PBS (supplemented to 3% (*W/V*) NaCl final concentration). One μL bacteria or OMV fractions were spotted onto 1% (*W/V*) PBS-agarose pad supplemented with 3% (*W/V*) NaCl. Fluorescence images were acquired with a Nikon Ti-2E inverted microscope using NIS-Elements AR 5.20.00 software and ImageJ was used for image analysis. Exposure time was 500 ms, the minimum and maximum displayed value of brightness and contrast were set at 3 200−3 500 for 2 h-induced-OMV samples and 10 000−15 000 for 5 h-induced-OMV samples.

1.10 Western blot

Protein samples of whole cell and OMVs were fractionated by 12% SDS-PAGE gel and transferred to PVDF membrane by electrophoresis. Membrane was blocked with 5% (*W/V*) non-fat milk in TBST buffer (50 mmol/L Tris, 150 mmol/L NaCl, 0.5% (*V/V*) Tween-20, pH 7.6) for 1 h at room temperature. Then the membrane was incubated with primary antibody (mouse monoclonal anti-GFP) in TBST with 1% (*W/V*) non-fat milk. The membrane was washed three times and incubated with anti-mouse IgG horseradish peroxidase (HRP)-conjugated secondary antibody in TBST with 1% (*W/V*) non-fat milk for 1 h followed by detection using ECL solution. The beta subunit of RNA polymerase (RpoB) was used as control for cell lysis. The secondary antibody goat anti-mouse IgG HRP and RpoB were used at 1:15 000 dilution, while anti-GFP primary antibody at 1:10 000.

2 Results and Analysis

2.1 Isolation of OMVs in different growth phases of *V. natriegens*

To determine whole cell and OMVs proteome composition during exponential phase growth, we first monitored bacterial growth in LB3 media and picked OD_{600}=0.5 and 1.5 as two sampling points (Figure 1A). The former is when inducers are often added for heterologous protein expression while the latter is when cells are exiting exponential phase growth. Using high-speed centrifugation, we collected OMVs and analyzed them using transmission electron microscopy (TEM) and dynamic light scattering

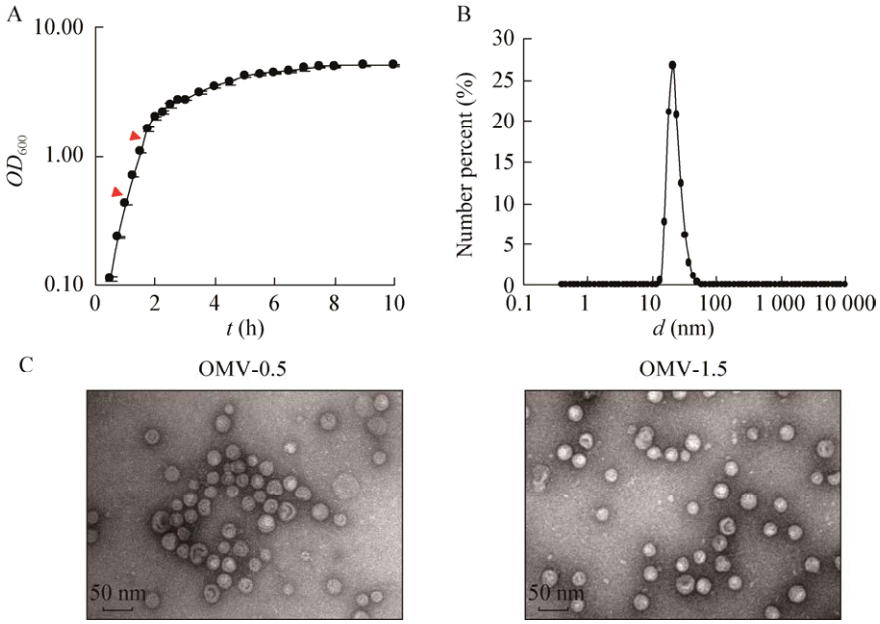

Figure 1 Characterization of growth and OMVs of *V. natriegens*

图 1 *V. natriegens* 生长情况及 OMV 的表征

Note: A: Growth curve of *V. natriegens* strain cultured at 37 °C in LB3 medium. Y axis was set to Log_{10} scale. Error bars indicate the mean ± standard deviation of three biological replicates. Arrows indicate the two specific time points of OD_{600}=0.5 and OD_{600}=1.5. B: Size distribution of the OMVs isolated from *V. natriegens*. OMVs were measured using DLS (dynamic light scattering). C: Transmission electron microscopy pictures of the OMVs isolated from *V. natriegens* in mid- and late-exponential phases

注：A：*V. natriegens* 在 37 °C、LB3 培养基中的生长曲线，Y 轴设置为 Log_{10} 比例，误差磅表示 3 个生物学重复的标准偏差，箭头表示 OD_{600}=0.5 和 OD_{600}=1.5 这 2 个特定时间点。B：从 *V. natriegens* 分离的 OMVs 的粒径分布，使用动态光散射(Dynamic Light Scattering，DLS)进行检测。C：从指数期中期和指数期末期 2 个时期(OD_{600}=0.5 和 OD_{600}=1.5)分离得到的 OMV 的透射电镜图

(DLS). Results show that the isolated OMVs were small, spherical particles with an average diameter of 25 nm (Figures 1B and 1C). The size of OMVs between OMV-0.5 and OMV-1.5 samples shows no difference under the observation of TEM and DLS. There were very few membrane debris, pili or fragments of flagella, indicating high quality of OMV preparation.

2.2 Overview of proteomic analysis of whole cell and OMVs from *V. natriegens*

Using LC-MS/MS, we analyzed protein profiles from whole cell and OMV samples. We identified 1 480 proteins of Cell-0.5, 1 565 proteins of Cell-1.5, 288 proteins of OMV-0.5 and 317 proteins of OMV-1.5 from three independent experiments. These identified proteins appeared in at least two of the three independent experiments, and all of them were predicted with subcellular locations. We identified 1 480 and 1 565 proteins in whole cell samples under mid- and late-exponential phases, of which 226 and 234 proteins were also found in OMV samples, respectively. A total of 185 proteins were present in all four groups, while 1 389 and 254 proteins were found in both mid and late whole cell samples and OMV samples, respectively (Figure 2A). In OMV-0.5 and OMV-1.5 samples, outer membrane, periplasmic, and extracellular proteins were enriched while about 37.15% and 29.97% were cytoplasmic proteins, respectively. In whole cell samples, more than 65% were cytoplasmic proteins (Figure 2B). We also performed prediction of subcellular locations on whole 4 688 proteins of *V. natriegens* which contained in proteome database of UniProt. The number of proteins in 6 groups, including outer membrane, periplasm, cytoplasm, cytoplasmic membrane, extracellular, and unknown, was taken as the theoretical number. The number of proteins with different locations in four samples (Cell-0.5, Cell-1.5, OMV-0.5, OMV-1.5) was compared with the theoretical number. Comparing with the theoretical number of each category in subcellular location, we identified about 40% of cytoplasmic proteins and a similar portion of periplasmic and outer membrane proteins in both whole cell samples (Figure 2C). OMV proteins are primarily made of outer membrane, periplasmic and extracellular proteins (Figure 2C). In addition, the proteomes of mid- and late-exponential phases share more than 80% identity for both whole cells (Cell-0.5 and Cell-1.5) and OMVs (OMV-0.5 and OMV-1.5), suggesting a relatively stable protein composition during exponential phase growth.

2.3 Functional cluster analysis of whole cell and OMV proteins

We functionally categorized all identified proteins using the GO database and KEGG pathway analyses. We found that proteins in whole cell and OMV samples were abundant in functional groups including cellular process, metabolic process, catalytic activity and binding (Figure 3). As expected, most proteins are involved in growth-related biological functions including metabolic enzymes, translation, and nutrient transport. Figure 4 shows the top 10 KEGG pathways, the most abundant of which are purine metabolism and two-component systems with 55 and 61 proteins in Cell-0.5 and Cell-1.5 samples, respectively. Metabolism of purine and pyrimidine nucleotides is essential for the biochemical processes of DNA and RNA synthesis. The proteins PurF, UPP, and GPT identified from whole cell samples are involved in nucleotide metabolism, for the synthesis of IMP, UMP, GMP and XMP[40-42]. Two-component systems control many functions including signaling, communication and adaptation, which are critical for bacteria to respond to environmental changes[43].

Cells growing in exponential phase express a large number of proteins involved in nucleotide and amino acid metabolism, and ribosomal functions to meet the growth demand. The identified top 10 KEGG pathways also contain glycolysis/gluconeogenesis, quorum sensing and biofilm formation. ATP-binding cassette (ABC) transporters are membrane proteins that use ATP hydrolysis to transport various molecules including peptides, ions, amino acids, sugars, polysaccharides, and lipids[44]. Notably, bacteria mainly use amino acids as nutrient source when growing in LB which contains low concentration of sugars[14]. Furthermore, more proteins involved in two-component system, quorum sensing and biofilm formation are present in Cell-1.5 sample than in Cell-0.5 sample, suggesting cells might be adjusting to increased density and depleted nutrients.

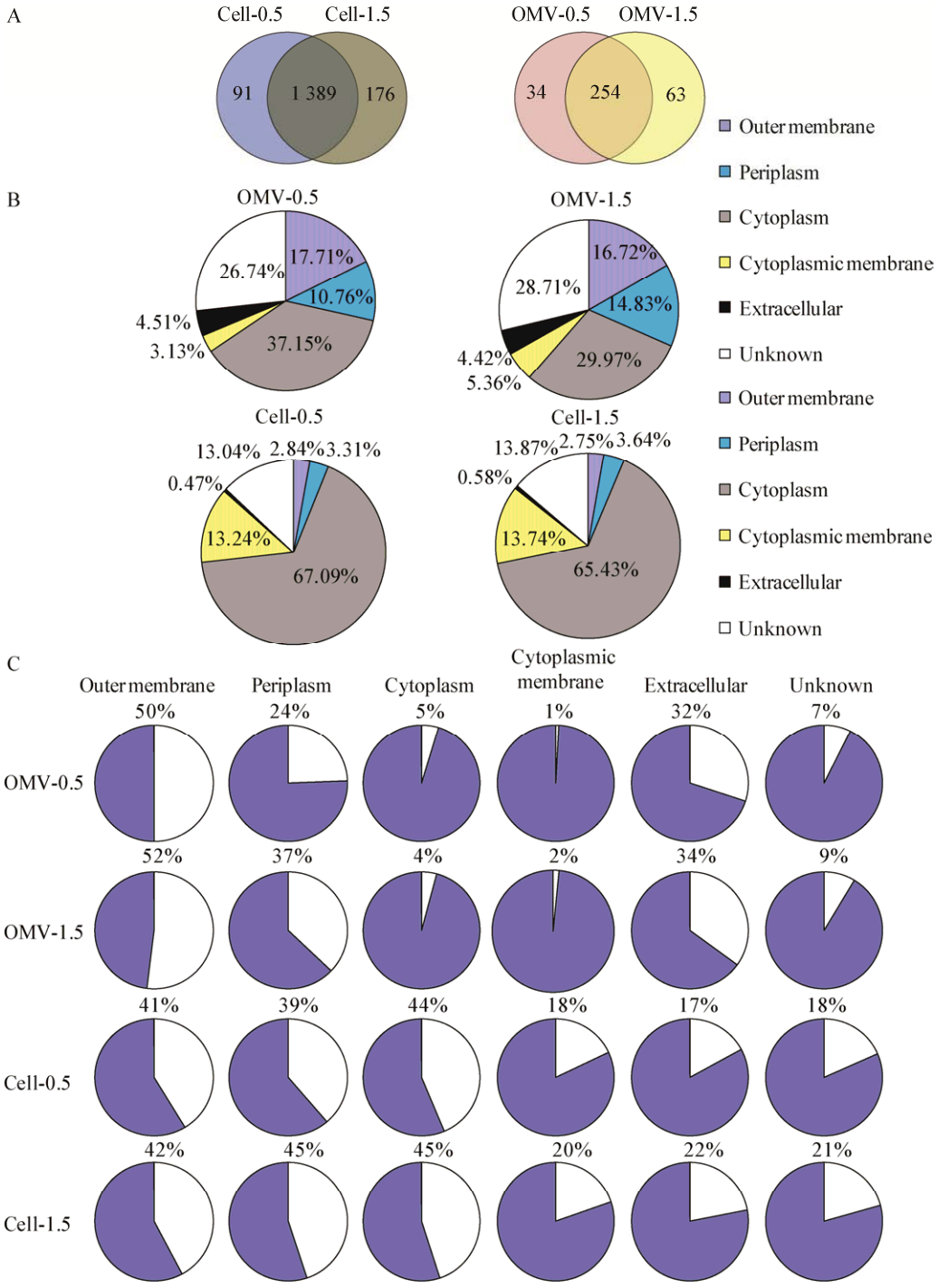

Figure 2 Proteomic analysis of whole cell and OMV samples by LC-MS/MS

图 2 全细胞与 OMV 样品的 LC-MS/MS 蛋白质组分析

Note: A: Venn diagrams of proteins in whole cell sample from mid-exponential phase (Cell-0.5), whole cell sample from late-exponential phase (Cell-1.5), OMVs isolated from mid-exponential phase (OMV-0.5), and OMVs isolated from late-exponential phase (OMV-1.5). B: Classification of identified proteins in whole cell and OMV samples from mid- and late-exponential phases based on predicted subcellular locations. C: Proportion of identified proteins to the whole theoretical proteome (white area indicates the proportion of identified proteins)

注：A：指数期中期全细胞样品(Cell-0.5)，指数期末期全细胞样品(Cell-1.5)，指数期中期 OMV (OMV-0.5)，指数期末期 OMV (OMV-1.5)的蛋白韦恩图。B：指数期中期和末期全细胞与 OMV 样品鉴定蛋白的亚细胞定位分类。C：鉴定蛋白与 *V. natriegens* 理论蛋白的百分比(白色区域表示鉴定蛋白的占比)

In OMVs, KEGG pathway analysis shows that several pathways including ABC transporters, flagellar assembly and two-component system are abundant in OMV-0.5 and OMV-1.5 samples (Figure 4). Notably, ribosomal proteins are also present in OMVs. The peptidoglycan-associated protein Pal and periplasmic protein TolB are parts of Tol-Pal system and found in the OMVs. The Tol-Pal complex controls outer membrane integrity and invagination during cell division[45]. Some cytoplasmic proteins including ribosomal proteins (RplA, RplB, RpsB, RpsC), chaperone proteins (GroL, DnaK, HtpG), DNA-directed RNA polymerase (RpoB, RpoC), elongation factor (FusA), and enzymes (pyruvate dehydrogenase, glutamine synthetase, aconitate hydratase, dihydrolipoyl dehydrogenase) were also identified in OMV samples of *V. natriegens*.

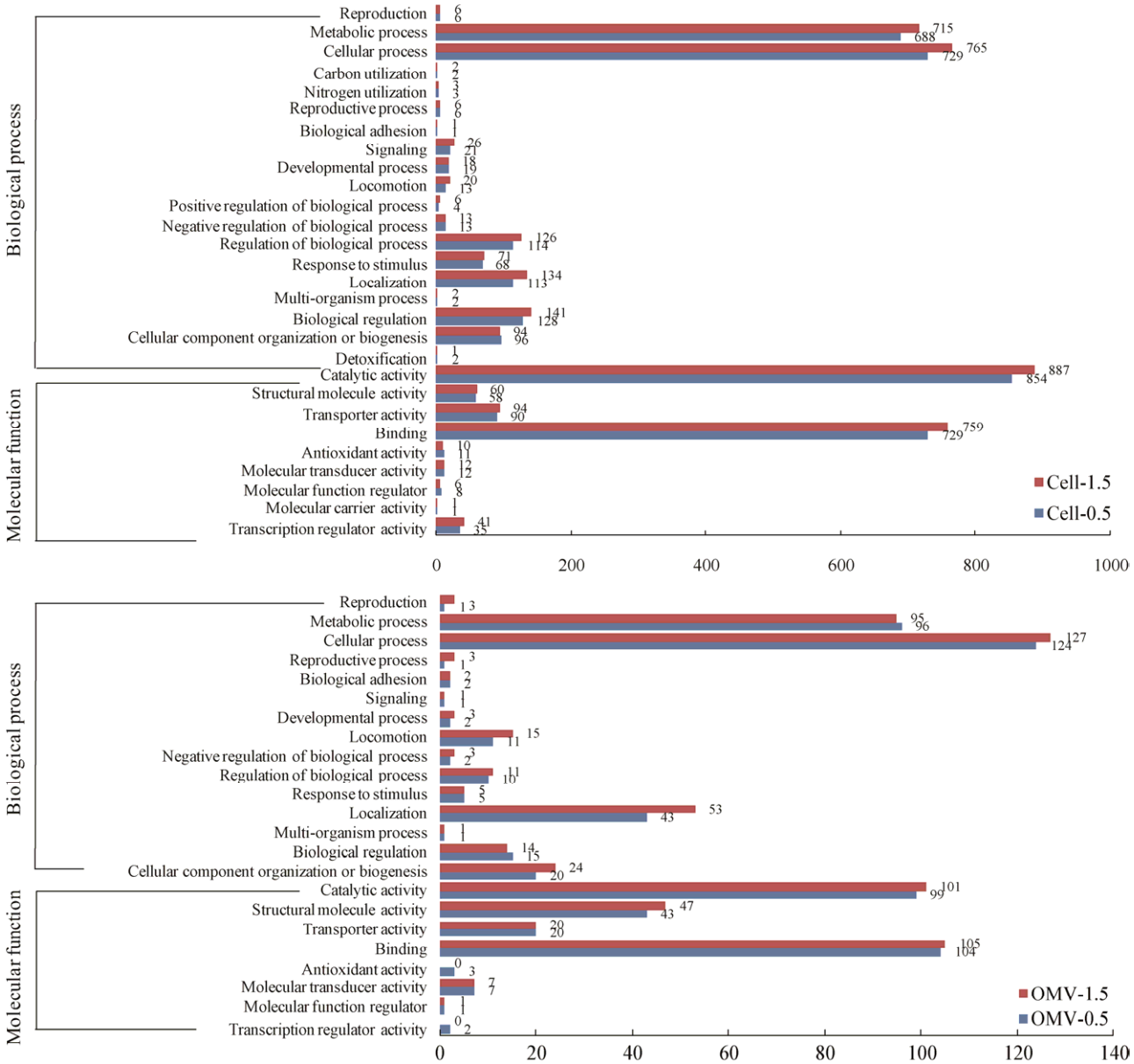

Figure 3 Distribution of the whole cell and OMV proteins classified into different GO terms
图 3 全细胞和 OMV 蛋白的 GO 注释分类

Note: The GO annotation is based on the second levels in biological processes (BP) and molecular functions (MF)
注：GO 注释基于生物过程(BP)与分子功能(MF)的二级分类

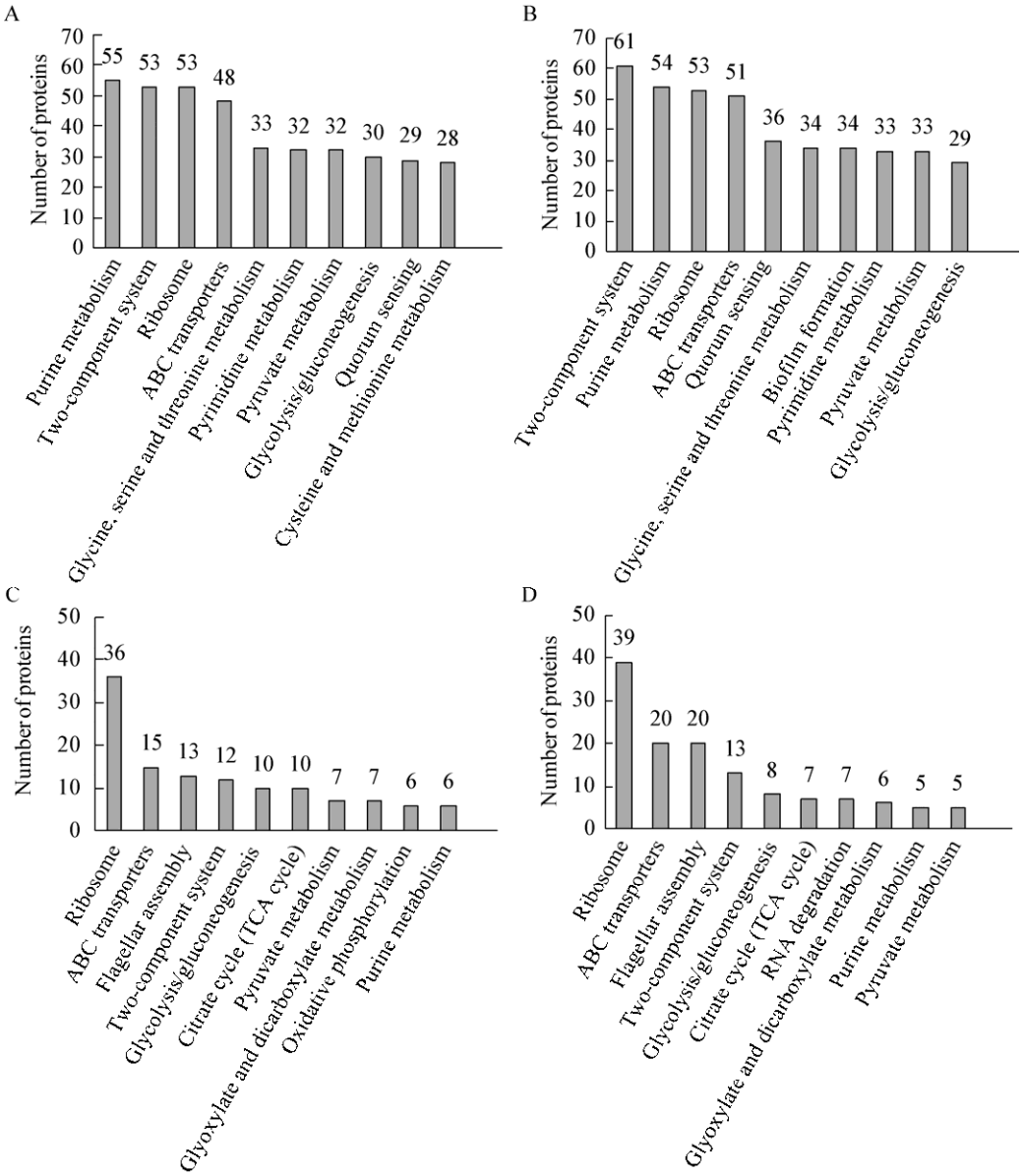

Figure 4 The top 10 KEGG pathways of identified proteins in whole cell and OMV samples
图 4 全细胞与 OMVs 样品中鉴定到的前 10 种 KEGG 通路

Note: A: Cell-0.5; B: Cell-1.5; C: OMV-0.5; D: OMV-1.5. Functional pathways annotated in KEGG are ranked based on the number of proteins
注：A：Cell-0.5；B：Cell-1.5；C：OMV-0.5；D：OMV-1.5。KEGG 注释的功能通路根据蛋白的数量进行排序

2.4 OmpA24-sfGFP fusion is enriched in outer membrane vesicles of *V. natriegens*

A main objective of OMV proteomic profiling is to find candidate carrier proteins in OMVs for delivery of heterologous proteins. The carrier protein should be stable in OMVs, especially in the rapid growth phase. Therefore, two time points OD_{600}=0.5 and OD_{600}=1.5 were chosen as the representatives of exponential phase to extract OMVs and identify the protein composition. From the proteomic results, we selected outer membrane proteins and periplasmic proteins that appeared in both mid- and late-exponential phases, and avoided enzymes and regulatory factors that may have pleiotropic effects. We selected 8 proteins (OmpW, TolC, OmpA24, Pal, MalE, TolB, Skp and PotD) as OMV carriers and employed sfGFP to make fusion protein with these carriers for the study of cargo protein delivery (Table 3). When these

constructs were induced using 0.1 mmol/L IPTG, we found different degrees of growth inhibition (Figure 5). So we changed to a lower dose of IPTG (0.001 mmol/L) and found that there was little effect on growth (Figure 5). We then analyzed expression of target proteins in bacterial cells and OMVs by Western blot and fluorescence microscopy analyses (Figures 6 and 7). All but the OmpW-sfGFP fusion proteins were detected in whole cell samples by Western blot analysis (Figure 6A). In OMV samples, only the OMV sample from pOmpA24 construct was detected by Western blot with an anti-GFP antibody (Figure 6B). Fluorescence microscopy analyses show that all constructs were expressed in cells, with all but TolB-sfGFP highlighting the membrane or periplasm (Figure 7).

Next, we focused on optimizing OMV-expression of the pOmpA24 construct. Because overexpression of the OmpA24-sfGFP fusion protein with 0.1 mmol/L IPTG showed growth inhibition, we lowered the inducer level to 0.001 mmol/L IPTG and extended induction time to 5 h. We found strong fluorescence signals of OmpA24-sfGFP in the OMV samples and confirmed its presence by Western blot and fluorescence microscopy analyses (Figures 8A and 8B). By comparison, plasmid-expressed sfGFP alone was not detected in OMV samples in either fluorescence microscopy or Western blot analyses. These results indicate that sfGFP can be packaged in OMVs of *V. natriegens* only when it is fused to OmpA24 but not on its own.

Table 3 Eight candidates with their subcellular locations
表 3 8 种候选蛋白及其亚细胞定位

Protein	Description	Subcellular location
OmpW	Outer membrane protein OmpW	Outer membrane
OmpA24	OmpA-like domain-containing protein	Outer membrane
TolC	Outer membrane channel protein TolC	Outer membrane
Pal	Peptidoglycan-associated protein	Outer membrane
TolB	Tol-Pal system protein TolB	Periplasm
MalE	Maltodextrin-binding protein	Periplasm
PotD	Putrescine-binding periplasmic protein	Periplasm
Skp	Chaperone protein Skp	Periplasm

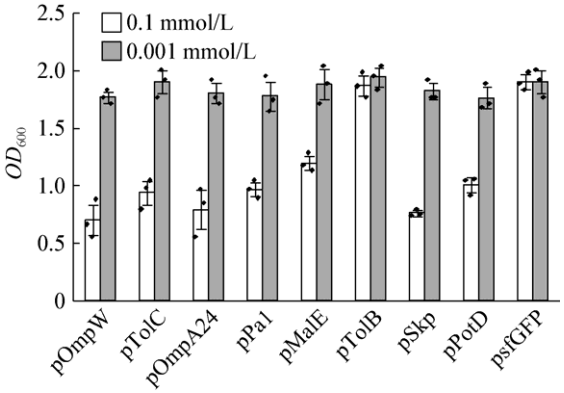

Figure 5 Growth inhibition of *V. natriegens* contained different pET-22b plasmids
图 5 含有不同 pET-22b 质粒的 *V. natriegens* 的生长抑制

Note: OD_{600} values of the strains which contained different pET-22b plasmids under 0.1 mmol/L and 0.001 mmol/L IPTG induction after 2 h. All the strains with plasmids began to be induced at OD_{600}=0.5
注：含有不同 pET-22b 表达质粒的细菌在 0.1 mmol/L 和 0.001 mmol/L IPTG 诱导剂浓度下诱导 2 h 后的 OD_{600} 值所有带质粒的细菌在 OD_{600}=0.5 时被诱导

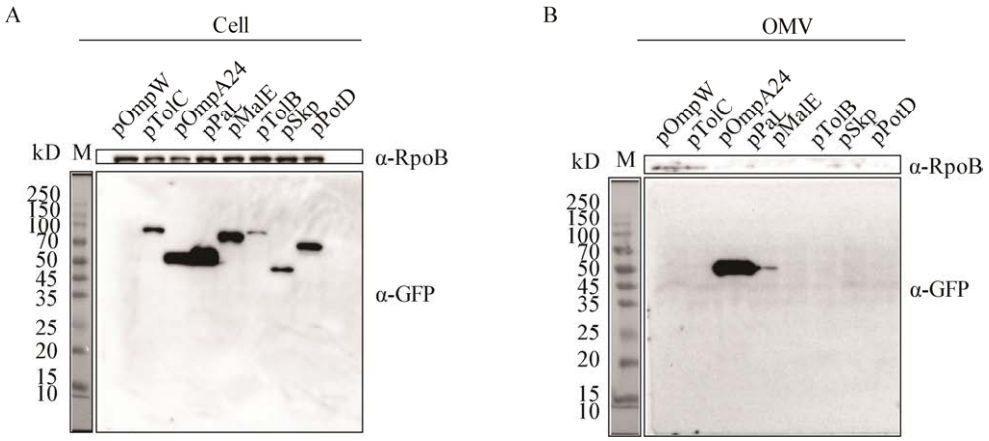

Figure 6 Western blot analysis of the expression of sfGFP fused proteins
图 6 sfGFP 融合蛋白的 Western blot 分析

Note: A: Whole cell samples; B: OMV samples. Proteins in whole cell samples and OMVs were subject to SDS-PAGE analysis, followed by Western blot analysis with anti-GFP antibody. The RNA polymerase subunit RpoB serves as a control for equal protein loading and cell lysis. Strains were induced with 0.001 mmol/L IPTG for 2 h
注：A：全细胞样品；B：OMV 样品。全细胞和 OMVs 的蛋白经 SDS-PAGE 分析，随后使用 GFP 抗体进行 Western blot 分析。RNA 聚合酶亚基 RpoB 作为对照用于比较相等的蛋白上样量和细胞裂解。0.001 mmol/L IPTG 诱导细菌 2 h

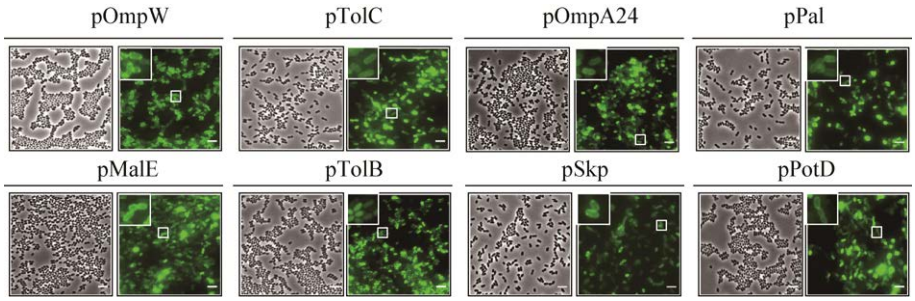

Figure 7 Fluorescence microscopy analysis of *V. natriegens* carrying pET-22b plasmids
图 7 携带 pET-22b 质粒的 *V. natriegens* 的荧光显微镜分析

Note: Fluorescence microscopic images (50 μm×50 μm) of *V. natriegens* carrying pET-22b plasmids. Strains were induced with 0.001 mmol/L IPTG for 2 h. Insets (5 μm×5 μm) in top left correspond to area in white boxes. Scale bars, 5 μm
注：含 pET-22b 质粒的 *V. natriegens* 荧光显微镜图像(50 μm×50 μm)。0.001 mmol/L IPTG 诱导细菌 2 h。左上角插图(5 μm×5 μm)对应于图像中白色方框区域。比例尺为 5 μm

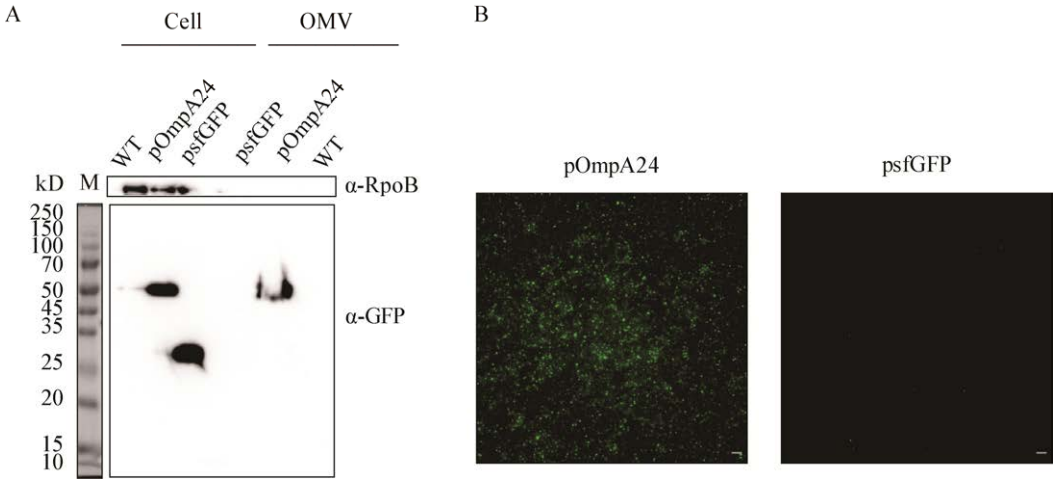

Figure 8 Western blot and fluorescence microscopy analyses of *V. natriegens*
图 8 *V. natriegens* 的 Western blot 和荧光显微镜分析

Note: A: Strains carrying pOmpA24 and psfGFP plasmids were induced with 0.001 mmol/L IPTG for 5 h. Proteins in whole cell samples and OMVs were subject to SDS-PAGE analysis, followed by Western blot analysis with anti-GFP antibody. The RNA polymerase subunit RpoB serves as a control for equal protein loading and cell lysis. Molecular weight marker (M) is annotated on the left. B: Fluorescence microscopic images (132 μm×132 μm) of OMVs isolated from *V. natriegens* carrying pOmpA24 and psfGFP plasmids. Strains were induced with 0.001 mmol/L IPTG for 5 h. Scale bars, 5 μm
注：A：0.001 mmol/L IPTG 诱导携带 pOmpA24 和 psfGFP 质粒的细菌 5 h。全细胞和 OMVs 的蛋白经 SDS-PAGE 分析，随后使用 GFP 抗体进行 Western blot 分析。RNA 聚合酶亚基 RpoB 作为对照用于比较相等的蛋白上样量和细胞裂解。蛋白分子量标记(M)展示在图左侧。B：分别从含 pOmpA24 和 psfGFP 质粒的 *V. natriegens* 中分离得到的 OMVs 的荧光显微镜图像(132 μm×132 μm)。0.001 mmol/L IPTG 诱导细菌 5 h，比例尺为 5 μm

2.5 OmpA24 is a conserved membrane protein in many species

OmpA24 contains an OmpA-like domain in its C-terminal and links to sfGFP with a linker. OmpA-like domain-containing proteins can anchor to the peptidoglycan and outer membrane by an N-terminal β-barrel; an N-terminal lipid anchor; or by binding to porins, which could stabilize the cell envelope and outer membrane integrity[46-50].

We next examined the distribution of OmpA24 (GenBank accession number: ANQ12348.1) using BLASTp, and found OmpA24 homologs are widely distributed in genera of *Vibrio*, *Aliivibrio*, and *Marinomonas*. We searched OmpA24 in non-redundant

protein database for its close homologs in *Vibrio* and in the non-redundant protein database excluding genera *Vibrio* to include more distant homologs. By ranking the hits by percent identity and excluding redundant species, we selected 20 representative sequences, 10 from each search. The sequence identities of the top 10 homologs in genera *Vibrio* are more than 88% and those of the 10 homologs from non-*Vibrio* species are more than 66%. Using phylogenetic tree and conserved domain analyses, we compared these 20 homologs with OmpA24 (Figures 9 and 10). OmpA24 is clustered with homologs from genera *Vibrio* and divergent from genera *Aliivibrio* and *Marinomonas*. Domain analysis shows that OmpA24 and its homologs exhibit conserved N-terminal glycine zipper domains and C-terminal OmpA family domains.

3 Discussion and Conclusion

In this study, we demonstrate that *V. natriegens* can produce OMVs throughout exponential growth and present the first proteomic snapshot of OMVs and related whole cell samples under different growth phases that are relevant to its application as a promising protein-expression tool. We identified 288, 317, 1 480, 1 565 proteins in OMV-0.5, OMV-1.5, Cell-0.5 and Cell-1.5, respectively. Results show that protein composition remains largely stable during exponential phase growth. By comparing a number of OMV proteins for heterologous sfGFP-fusion cargo enrichment, we show that OmpA24 is the most efficient as a fusion carrier.

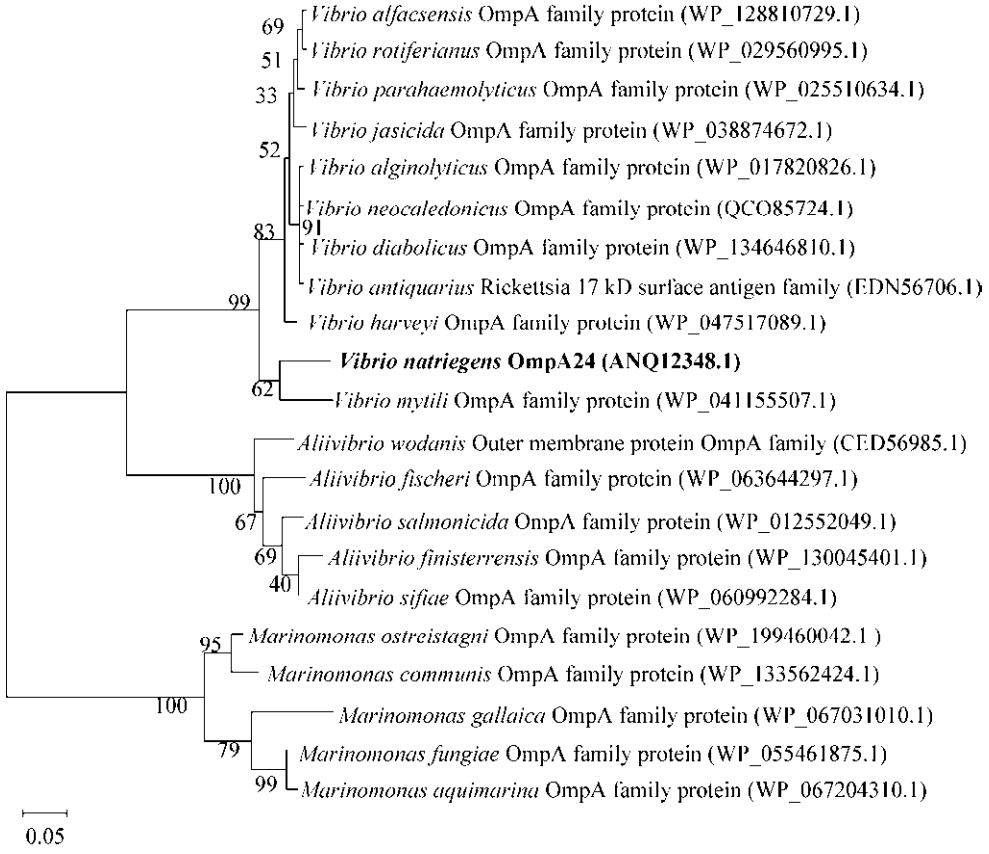

Figure 9 Maximum-likelihood phylogeny of OmpA24 and 20 homologs
图 9 最大似然法进化分析 OmpA24 及 20 个同源蛋白

Note: The phylogenetic tree was constructed using MEGA X software. Protein experimentally tested in this study is highlighted in bold. Numbers in parentheses represent the accession numbers in GenBank of OmpA24 and 20 homologs, numbers on the branches refer to the confidence and the bar (0.05) represents the evolution distance
注：进化树通过 MEGA X 软件生成。本实验研究的蛋白用粗体突出显示。括号内为 OmpA24 及其 20 个同源蛋白的 GenBank 登录号，分支点上的数字表示置信度，标尺值(0.05)代表进化距离

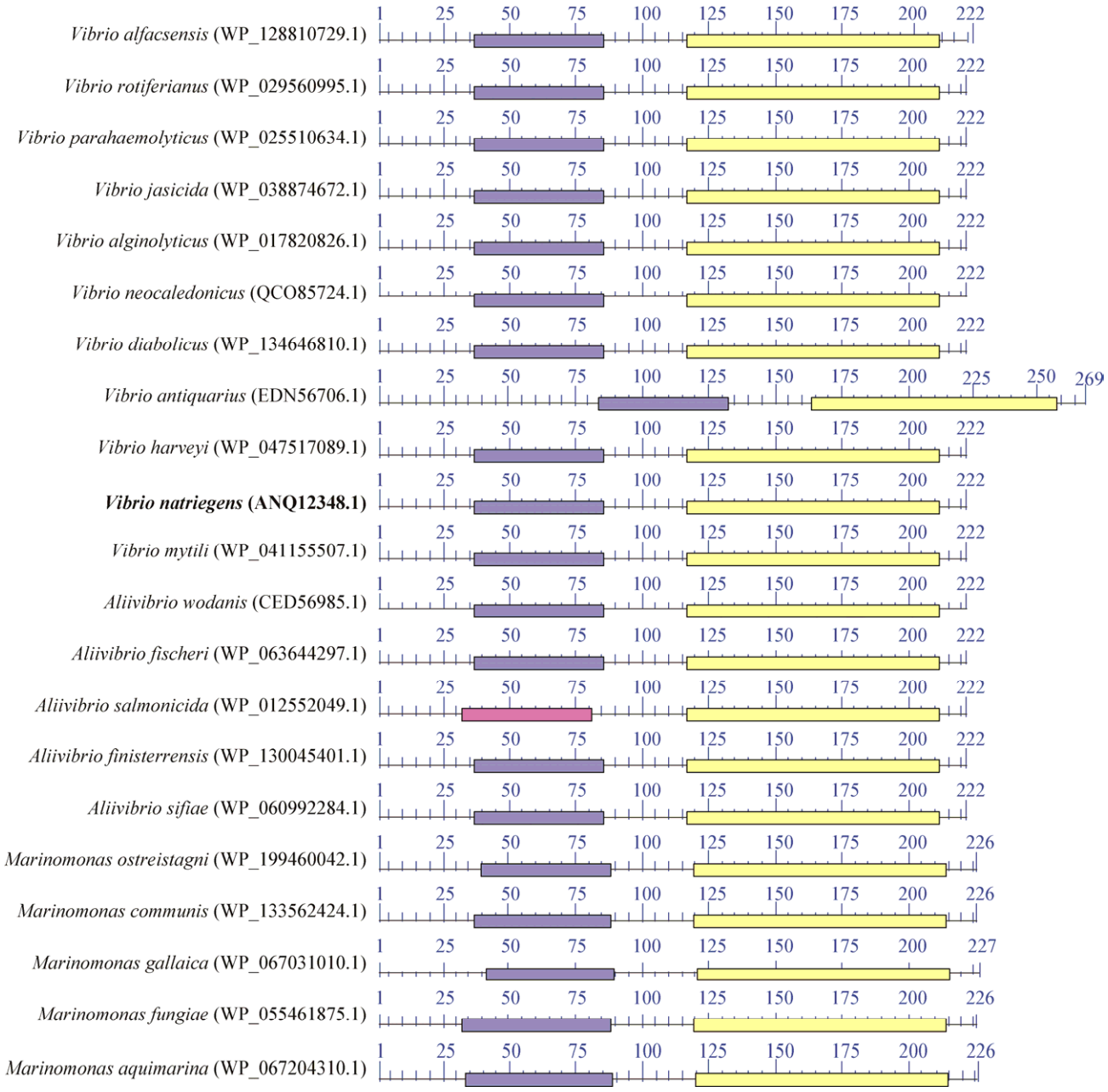

Figure 10 Conserved domain analysis of OmpA24 and 20 homologs
图 10 OmpA24 及 20 个同源蛋白的保守结构域分析

Note: Domain analysis was performed using PfamScan tool with default settings. Purple color indicates the glycine zipper domain. Pink color indicates the YMGG-like glycine zipper domain. Yellow color indicates the OmpA family domain
注：利用 PfamScan 工具进行结构域分析，参数设置采用默认值。紫色表示甘氨酸链式结构域，粉色表示 YMGG-类甘氨酸链式结构域，黄色表示 OmpA 家族结构域

Some cytoplasmic proteins and cytoplasmic membrane proteins were identified in OMVs of *V. natriegens* in this study. Notably, some cytoplasmic proteins identified in our OMVs were also observed in the OMVs of other bacteria including *A. baumannii*, *Francisella novicida* and *Francisella philomiragia*[36,51]. Besides ribosomal proteins, DNA and RNA have also been identified in OMVs of other

bacteria[20,52,53]. A previous study examining the membrane vesicles of *Pseudomonas aeruginosa* has reported a cell-lysis-mediated mechanism to account for the presence of cytosolic components[54]. However, it remains debatable whether these cytosolic contents play important physiological roles.

Almost all Gram-negative bacteria produce OMVs, *V. natriegens* grows among the fastest[9,55-57]. A large amount of OMVs may be harvested in shorter time possibly, which makes *V. natriegens* a promising tool for OMVs application. OMVs have been used for multiple applications. For example, OMVs isolated from *A. baumannii*, *Bordetella pertussis* and *Burkholderia pseudomallei*, can evoke antibody responses in animal models, and the Meningitis type B OMV vaccine has been approved for clinical application[58-62]. OMVs have also been used in transdermal nanoplatforms for inducing tumor-targeting drug delivery, in activation of the caspase-11-GSDMD pathway to disperse intravascular coagulation, and in modulating host immune systems[63-66]. Here, we established a method for extracting OMVs and characterized its proteomic composition. We report that OmpA24-sfGFP can be found in OMVs with the highest efficiency of all fusion proteins tested. Notably, a high induction level of the OmpA24-sfGFP fusion protein showed bacterial growth inhibition. This may be due to the induced levels of OmpA24-sfGFP protein disturbing OmpA24-mediated interaction with peptidoglycan and outer membrane. Although this problem could be mitigated by lowering the induction, optimization using mutagenesis and growth conditions may be needed to further increase yield in future studies.

In summary, our study provides a general understanding of the protein composition of *V. natriegens* whole cells and OMVs during exponential-phase growth. We demonstrate an OMV-protein OmpA24 is a promising carrier for delivering sfGFP as a protein-fusion cargo to the OMVs. Using similar tools and techniques, we can use the OMVs of *V. natriegens* to deliver antigens or drugs for a variety of biotechnological applications.

REFERENCES

[1] Gopal GJ, Kumar A. Strategies for the production of recombinant protein in *Escherichia coli*[J]. Protein Journal, 2013, 32(6): 419-425

[2] Zahrl RJ, Peña DA, Mattanovich D, Gasser B. Systems biotechnology for protein production in *Pichia pastoris*[J]. FEMS Yeast Research, 2017, 17(7): fox068

[3] Weinstock MT, Hesek ED, Wilson CM, Gibson DG. *Vibrio natriegens* as a fast-growing host for molecular biology[J]. Nature Methods, 2016, 13(10): 849-851

[4] Lee HH, Ostrov N, Gold MA, Church GM. Recombineering in *Vibrio natriegens*[EB/OL]. bioRxiv, 2017

[5] Lee HH, Ostrov N, Wong BG, Gold MA, Khalil AS, Church GM. Functional genomics of the rapidly replicating bacterium *Vibrio natriegens* by CRISPRi[J]. Nature Microbiology, 2019, 4(7): 1105-1113

[6] Ellis GA, Tschirhart T, Spangler J, Walper SA, Medintz IL, Vora GJ. Exploiting the feedstock flexibility of the emergent synthetic biology chassis *Vibrio natriegens* for engineered natural product production[J]. Marine Drugs, 2019, 17(12): 679

[7] Schleicher L, Muras V, Claussen B, Pfannstiel J, Blombach B, Dibrov P, Fritz G, Steuber J. *Vibrio natriegens* as host for expression of multisubunit membrane protein complexes[J]. Frontiers in Microbiology, 2018, 9: 2537

[8] Wiegand DJ, Lee HH, Ostrov N, Church GM. Cell-free protein expression using the rapidly growing bacterium *Vibrio natriegens*[J]. Journal of Visualized Experiments, 2019(145)

[9] Hoff J, Daniel B, Stukenberg D, Thuronyi BW, Waldminghaus T, Fritz G. *Vibrio natriegens*: an ultrafast-growing marine bacterium as emerging synthetic biology chassis[J]. Environmental Microbiology, 2020, 22(10): 4394-4408

[10] Rolfe MD, Rice CJ, Lucchini S, Pin C, Thompson A, Cameron AD, Alston M, Stringer MF, Betts RP, Baranyi J, et al. Lag phase is a distinct growth phase that prepares bacteria for exponential growth and involves transient metal accumulation[J]. Journal of Bacteriology, 2012, 194(3): 686-701

[11] Baranyi J, Roberts TA. Principles and application of predictive modeling of the effects of preservative factors on microorganisms, p342-358. In Lund BM, Baird-Parker TC, Gould GW (ed), the microbiological safety and quality of food[J]. Aspen, Gaithersburg, MD. 2000

[12] Navarro Llorens JM, Tormo A, Martínez-García E. Stationary phase in Gram-negative bacteria[J]. FEMS Microbiology Reviews, 2010, 34(4): 476-495

[13] Finkel SE. Long-term survival during stationary phase: evolution and the GASP phenotype[J]. Nature Reviews Microbiology, 2006, 4(2): 113-120

[14] Sezonov G, Joseleau-Petit D, D'Ari R. *Escherichia coli* physiology in Luria-Bertani broth[J]. Journal of Bacteriology, 2007, 189(23): 8746-8749

[15] Lee EY, Choi DS, Kim KP, Gho YS. Proteomics in Gram-negative bacterial outer membrane vesicles[J]. Mass Spectrometry Reviews, 2008, 27(6): 535-555

[16] Kulkarni HM, Jagannadham MV. Biogenesis and multifaceted roles of outer membrane vesicles from

Gram-negative bacteria[J]. Microbiology (Reading), 2014, 160(Pt 10): 2109-2121

[17] Horstman AL, Kuehn MJ. Enterotoxigenic *Escherichia coli* secretes active heat-labile enterotoxin via outer membrane vesicles[J]. Journal of Biological Chemistry, 2000, 275(17): 12489-12496

[18] Dorward DW, Garon CF, Judd RC. Export and intercellular transfer of DNA via membrane blebs of *Neisseria gonorrhoeae*[J]. Journal of Bacteriology, 1989, 171(5): 2499-2505

[19] Dorward DW, Garon CF. DNA is packaged within membrane-derived vesicles of Gram-negative but not Gram-positive bacteria[J]. Applied and Environmental Microbiology, 1990, 56(6): 1960-1962

[20] Sjöström AE, Sandblad L, Uhlin BE, Wai SN. Membrane vesicle-mediated release of bacterial RNA[J]. Scientific Reports, 2015, 5: 15329

[21] Elhenawy W, Debelyy MO, Feldman MF. Preferential packing of acidic glycosidases and proteases into *Bacteroides* outer membrane vesicles[J]. mBio, 2014, 5(2): e00909-e00914

[22] Lappann M, Otto A, Becher D, Vogel U. Comparative proteome analysis of spontaneous outer membrane vesicles and purified outer membranes of *Neisseria meningitidis*[J]. Journal of Bacteriology, 2013, 195(19): 4425-4435

[23] Baumgarten T, Sperling S, Seifert J, Von Bergen M, Steiniger F, Wick LY, Heipieper HJ. Membrane vesicle formation as a multiple-stress response mechanism enhances *Pseudomonas putida* DOT-T1E cell surface hydrophobicity and biofilm formation[J]. Applied and Environmental Microbiology, 2012, 78(17): 6217-6224

[24] Mashburn LM, Whiteley M. Membrane vesicles traffic signals and facilitate group activities in a prokaryote[J]. Nature, 2005, 437(7057): 422-425

[25] Yoon H, Ansong C, Adkins JN, Heffron F. Discovery of *Salmonella* virulence factors translocated via outer membrane vesicles to murine macrophages[J]. Infection and Immunity, 2011, 79(6): 2182-2192

[26] Ellis TN, Kuehn MJ. Virulence and immunomodulatory roles of bacterial outer membrane vesicles[J]. Microbiology and Molecular Biology Reviews, 2010, 74(1): 81-94

[27] Wang SH, Gao J, Wang ZJ. Outer membrane vesicles for vaccination and targeted drug delivery[J]. Wiley Interdisciplinary Reviews Nanomedicine and Nanobiotechnology, 2019, 11(2): e1523

[28] Kim JY, Doody AM, Chen DJ, Cremona GH, Shuler ML, Putnam D, DeLisa MP. Engineered bacterial outer membrane vesicles with enhanced functionality[J]. Journal of Molecular Biology, 2008, 380(1): 51-66

[29] Schroeder J, Aebischer T. Recombinant outer membrane vesicles to augment antigen-specific live vaccine responses[J]. Vaccine, 2009, 27(48): 6748-6754

[30] Daleke-Schermerhorn MH, Felix T, Soprova Z, Ten Hagen-Jongman CM, Vikström D, Majlessi L, Beskers J, Follmann F, De Punder K, Van Der Wel NN, et al. Decoration of outer membrane vesicles with multiple antigens by using an autotransporter approach[J]. Applied and Environmental Microbiology, 2014, 80(18): 5854-5865

[31] Liu JJ, Hsieh CL, Gelincik O, Devolder B, Sei S, Zhang S, Lipkin SM, Chang YF. Proteomic characterization of outer membrane vesicles from gut mucosa-derived *Fusobacterium nucleatum*[J]. Journal of Proteomics, 2019, 195: 125-137

[32] Kulkarni HM, Swamy CVB, Jagannadham MV. Molecular characterization and functional analysis of outer membrane vesicles from the Antarctic bacterium *Pseudomonas syringae* suggest a possible response to environmental conditions[J]. Journal of Proteome Research, 2014, 13(3): 1345-1358

[33] Mullaney E, Brown PA, Smith SM, Botting CH, Yamaoka YY, Terres AM, Kelleher DP, Windle HJ. Proteomic and functional characterization of the outer membrane vesicles from the gastric pathogen *Helicobacter pylori*[J]. Proteomics Clinical Applications, 2009, 3(7): 785-796

[34] Jang KS, Sweredoski MJ, Graham RLJ, Hess S, Clemons WM Jr. Comprehensive proteomic profiling of outer membrane vesicles from *Campylobacter jejuni*[J]. Journal of Proteomics, 2014, 98: 90-98

[35] Sidhu VK, Vorhölter FJ, Niehaus K, Watt SA. Analysis of outer membrane vesicle associated proteins isolated from the plant pathogenic bacterium *Xanthomonas campestris* pv. campestris[J]. BMC Microbiology, 2008, 8: 87

[36] Kwon SO, Gho YS, Lee JC, Kim SI. Proteome analysis of outer membrane vesicles from a clinical *Acinetobacter baumannii* isolate[J]. FEMS Microbiology Letters, 2009, 297(2): 150-156

[37] Lee EY, Bang JY, Park GW, Choi DS, Kang JS, Kim HJ, Park KS, Lee JO, Kim YK, Kwon KH, et al. Global proteomic profiling of native outer membrane vesicles derived from *Escherichia coli*[J]. Proteomics, 2007, 7(17): 3143-3153

[38] Donnarumma D, Maestri C, Giammarinaro PI, Capriotti L, Bartolini E, Veggi D, Petracca R, Scarselli M, Norais N. Native state organization of outer membrane porins unraveled by HDx-MS[J]. Journal of Proteome Research, 2018, 17(5): 1794-1800

[39] Kumar S, Stecher G, Li M, Knyaz C, Tamura K. MEGA X: molecular evolutionary genetics analysis across computing platforms[J]. Molecular Biology and Evolution, 2018, 35(6): 1547-1549

[40] Messenger LJ, Zalkin H. Glutamine phosphoribosylpyrophosphate amidotransferase from *Escherichia coli*. Purification and properties[J]. Journal of Biological Chemistry, 1979, 254(9): 3382-3392

[41] Jensen KF, Mygind B. Different oligomeric states are involved in the allosteric behavior of uracil phosphoribosyltransferase from *Escherichia coli*[J]. European Journal of Biochemistry, 1996, 240(3): 637-645

[42] Vos S, De Jersey J, Martin JL. Crystal structure of *Escherichia coli* xanthine phosphoribosyltransferase[J]. Biochemistry, 1997, 36(14): 4125-4134

[43] Stock AM, Robinson VL, Goudreau PN. Two-component signal transduction[J]. Annual Review of Biochemistry, 2000, 69: 183-215

[44] Jones PM, George AM. The ABC transporter structure and mechanism: perspectives on recent research[J]. Cellular and Molecular Life Sciences, 2004, 61(6): 682-699

[45] Gerding MA, Ogata Y, Pecora ND, Niki H, De Boer PAJ. The trans-envelope Tol-Pal complex is part of the cell division machinery and required for proper outer-membrane invagination during cell constriction in *E. coli*[J]. Molecular Microbiology, 2007, 63(4): 1008-1025

[46] Confer AW, Ayalew S. The OmpA family of proteins: roles in bacterial pathogenesis and immunity[J]. Veterinary Microbiology, 2013, 163(3-4): 207-222

[47] Grizot S, Buchanan SK. Structure of the OmpA-like domain of RmpM from *Neisseria meningitidis*[J]. Molecular Microbiology, 2004, 51(4): 1027-1037

[48] Volokhina EB, Beckers F, Tommassen J, Bos MP. The beta-barrel outer membrane protein assembly complex of *Neisseria meningitidis*[J]. Journal of Bacteriology, 2009, 191(22): 7074-7085

[49] Bouveret E, Bénédetti H, Rigal A, Loret E, Lazdunski C. *In vitro* characterization of peptidoglycan-associated lipoprotein (PAL)-peptidoglycan and PAL-TolB interactions[J]. Journal of Bacteriology, 1999, 181(20): 6306-6311

[50] Park JS, Lee WC, Yeo KJ, Ryu KS, Kumarasiri M, Hesek D, Lee M, Mobashery S, Song JH, Kim SI, et al. Mechanism of anchoring of OmpA protein to the cell wall peptidoglycan of the Gram-negative bacterial outer membrane[J]. FASEB Journal: Official Publication of the Federation of American Societies for Experimental Biology, 2012, 26(1): 219-228

[51] Pierson T, Matrakas D, Taylor YU, Manyam G, Morozov VN, Zhou WD, Van Hoek ML. Proteomic characterization and functional analysis of outer membrane vesicles of *Francisella novicida* suggests possible role in virulence and use as a vaccine[J]. Journal of Proteome Research, 2011, 10(3): 954-967

[52] Pérez-Cruz C, Carrión O, Delgado L, Martinez G, López-Iglesias C, Mercade E. New type of outer membrane vesicle produced by the Gram-negative bacterium *Shewanella vesiculosa* M7T: implications for DNA content[J]. Applied and Environmental Microbiology, 2013, 79(6): 1874-1881

[53] Yaron S, Kolling GL, Simon L, Matthews KR. Vesicle-mediated transfer of virulence genes from *Escherichia coli* O157: H7 to other enteric bacteria[J]. Applied and Environmental Microbiology, 2000, 66(10): 4414-4420

[54] Turnbull L, Toyofuku M, Hynen AL, Kurosawa M, Pessi G, Petty NK, Osvath SR, Cárcamo-Oyarce G, Gloag ES, Shimoni R, et al. Explosive cell lysis as a mechanism for the biogenesis of bacterial membrane vesicles and biofilms[J]. Nature Communications, 2016, 7: 11220

[55] Schwechheimer C, Kuehn MJ. Outer-membrane vesicles from Gram-negative bacteria: biogenesis and functions[J]. Nature Reviews Microbiology, 2015, 13(10): 605-619

[56] Schwechheimer C, Sullivan CJ, Kuehn MJ. Envelope control of outer membrane vesicle production in Gram-negative bacteria[J]. Biochemistry, 2013, 52(18): 3031-3040

[57] Kulp A, Kuehn MJ. Biological functions and biogenesis of secreted bacterial outer membrane vesicles[J]. Annual Review of Microbiology, 2010, 64: 163-184

[58] Van Der Pol L, Stork M, Van Der Ley P. Outer membrane vesicles as platform vaccine technology[J]. Biotechnology Journal, 2015, 10(11): 1689-1706

[59] McConnell MJ, Rumbo C, Bou G, Pachón J. Outer membrane vesicles as an acellular vaccine against *Acinetobacter baumannii*[J]. Vaccine, 2011, 29(34): 5705-5710

[60] Roberts R, Moreno G, Bottero D, Gaillard ME, Fingermann M, Graieb A, Rumbo M, Hozbor D. Outer membrane vesicles as acellular vaccine against pertussis[J]. Vaccine, 2008, 26(36): 4639-4646

[61] Nieves W, Petersen H, Judy BM, Blumentritt CA, Russell-Lodrigue K, Roy CJ, Torres AG, Morici LA. A *Burkholderia pseudomallei* outer membrane vesicle vaccine provides protection against lethal sepsis[J]. Clinical and Vaccine Immunology, 2014, 21(5): 747-754

[62] O'Ryan M, Stoddard J, Toneatto D, Wassil J, Dull PM. A multi-component meningococcal serogroup B vaccine (4CMenB): the clinical development program[J]. Drugs, 2014, 74(1): 15-30

[63] Peng LH, Wang MZ, Chu Y, Zhang L, Niu J, Shao HT, Yuan TJ, Jiang ZH, Gao JQ, Ning XH. Engineering bacterial outer membrane vesicles as transdermal nanoplatforms for photo-TRAIL-programmed therapy against melanoma[J]. Science Advances, 2020, 6(27): eaba2735

[64] Gu TW, Wang MZ, Niu J, Chu Y, Guo KR, Peng LH. Outer membrane vesicles derived from *E. coli* as novel vehicles for transdermal and tumor targeting delivery[J]. Nanoscale, 2020, 12(36): 18965-18977

[65] Peng Y, Gao M, Liu YK, Qiu XH, Cheng XY, Yang XY, Chen FP, Wang EH. Bacterial outer membrane vesicles induce disseminated intravascular coagulation through the caspase-11-gasdermin D pathway[J]. Thrombosis Research, 2020, 196: 159-166

[66] Hu RJ, Lin H, Li J, Zhao YZ, Wang MM, Sun XQ, Min YN, Gao YP, Yang MM. Probiotic *Escherichia coli* Nissle 1917-derived outer membrane vesicles enhance immunomodulation and antimicrobial activity in $RAW_{264.7}$ macrophages[J]. BMC Microbiology, 2020, 20(1): 268